International Urogynecology Journal (2019) 30:1305–1312
https://doi.org/10.1007/s00192-018-3704-5

ORIGINAL ARTICLE

Technique development and measurement of cross-sectional area of the pubovisceral muscle on MRI scans of living women

Mariana Masteling[1] · James A. Ashton-Miller[1] · John O. L. DeLancey[2]

Received: 20 February 2018 / Accepted: 18 June 2018 / Published online: 5 July 2018
© The International Urogynecological Association 2018

Abstract

Introduction and hypothesis Measurements of the anatomic cross-sectional area (CSA) of the pubovisceral muscle (PVM) in women are confounded by the difficulty of separating the muscle from the adjacent puborectal (PRM) and iliococcygeal (ICM) muscles when visualized in a plane orthogonal to the fiber direction. We tested the hypothesis that it might be possible to measure the PVM CSA within a defined region of interest based on magnetic resonance images (MRI).

Methods MRI scans of 11 women with unilateral PVM tears and seven primiparous women with intact muscles following elective C-section were used to identify the PVM injury zone defined by the mean location of its boundaries with the adjacent intact PRM and ICM from existing anatomic reference points using 3D Slicer and ImageJ software. Then, from the 15 or more 2-mm transverse slices available, the slice with the maximum anatomic CSA of the left and right PVM was found in 24 primiparous women with bilaterally intact muscles who had delivered via C-section.

Results Mean [± standard deviation (SD)] of the maximum left or right PVM cross-section areas for the 24 women, measured by two different raters, was 1.25 ± 0.29 cm^2 (range 0.75–1.86). The 5th, 50th, and 95th percentile values were 0.77, 1.23, and 1.80 cm^2, respectively. Inter- and intrarater measurement repeatability intraclass correlation coefficients exceeded 0.89 and 0.90, respectively.

Conclusions It is possible to use MRI to identify the volume of interest with the maximum anatomic cross section of the PVM belly while minimizing the inadvertent inclusion of adjacent PRM or ICM in that measurement.

Keywords Cross-sectional area · MRI · Pubovisceral muscle

Introduction

The levator ani muscles form the pelvic floor supporting the abdominal and pelvic organs within the pelvis. In women, this floor contains a hiatus through which the pelvic organs pass and through which the pelvic organs can prolapse (for review, see [1]). The pubovisceral portion of the levator ani (also known as the pubococcygeal muscle) originates bilaterally from the pubic rami on either side of the pubic symphysis and inserts into the lateral walls of the pelvic organs and perineal body [2]. It maintains a constant muscle tone to facilitate hiatal closure, providing additional tone to ensure closure during increases in intra-abdominal pressure [3].

Magnetic resonance imaging (MRI) examination of the levator in women with and without prolapse has shown that 55% of women with pelvic organ prolapse (POP) display evidence of a major obstetrical tear (defined as >50% missing muscle) in the pubovisceral muscle (PVM) compared with only 16% of women with normal support [4]. Using ultrasound (US), Dietz and Simpson found similar results and reported that 60% of women with uterine prolapse but only 14% of women without prolapse have some degree of tear [5]. The impaired action of this muscle renders it incapable of counteracting forces imposed on the hiatus by abdominal pressure, an imbalance that can eventually result in prolapse of the pelvic organs [6]. However, a woman with a naturally bulky PVM might lose 25% of her muscle to a type 1 tear [7] but still have more muscle than a woman with an intact but inherently small muscle. So, it seems desirable to accurately quantify the amount of PVM present in a given individual. Functionally, whether or not there is a tear, the amount of

✉ Mariana Masteling
mastelin@umich.edu

[1] Department of Mechanical Engineering, University of Michigan, 2350 Hayward St, Ann Arbor, MI 48109, USA

[2] Department of Obstetrics and Gynecology, University of Michigan, Ann Arbor, MI 48109, USA

muscle—specifically, the maximum anatomic cross-sectional area (CSA) of the muscle perpendicular to the fiber direction—on that side of the body determines how much force that the muscle can generate.

Both US and MRI have been used to measure PVM thickness [8, 9]. Muscle physiologists always estimate the maximum force-generation capability of a parallel fibered striated muscle under isometric conditions by measuring its anatomic CSA taken perpendicularly to the fibers [10], not its thickness. For example, a hypothetical rectangular cross-sectioned muscle 1-cm thick by 2-cm wide (having a CSA of 2 cm^2) will develop twice as much isometric force as a 1-cm-thick muscle that is 1-cm wide (CSA: 1 cm^2). So, one can see that thickness alone is not sufficient to determine a muscle's force-generating capacity. We therefore measured anatomic CSA, not thickness. In addition, CSA needs to be measured in the muscle belly, at the point where the CSA of the muscle is largest (Fig. 1). Although PVM CSA has been estimated by first making a 3D model of the muscle and then sectioning it [11], this laborious process introduces potential errors at many steps in model construction. It would therefore be preferable to make CSA measurements from the original MRI, not the model. In addition, the problem that several regions of the PVM are overlapped by the puborectal (PRM) or iliococcygeal (ICM) muscle, thereby complicating measurement of PVM CSA, has not been addressed.

The goal of this study, therefore, was to develop a technique directly from MRI to measure maximum CSA of muscle subdivision in the PVM injury zone in women with or without muscle tears and report the range variation found in its CSA in a cohort of 24 primiparous women, along with inter- and intrarater reliability. We tested the hypothesis that it is possible to identify the extent of the injury zone in 3D from existing landmarks in a convenience sample of women with unilateral tears, thereby yielding the dimensions of the region of interest (ROI) within which to seek the maximum anatomic CSA of the intact PVM directly from the MRI scan. We also tested the hypothesis that the coefficient of variation (CV) in the measured PVM CSA is similar, at 25%, to that found in other small, parallel-fibered, striated muscles in the body.

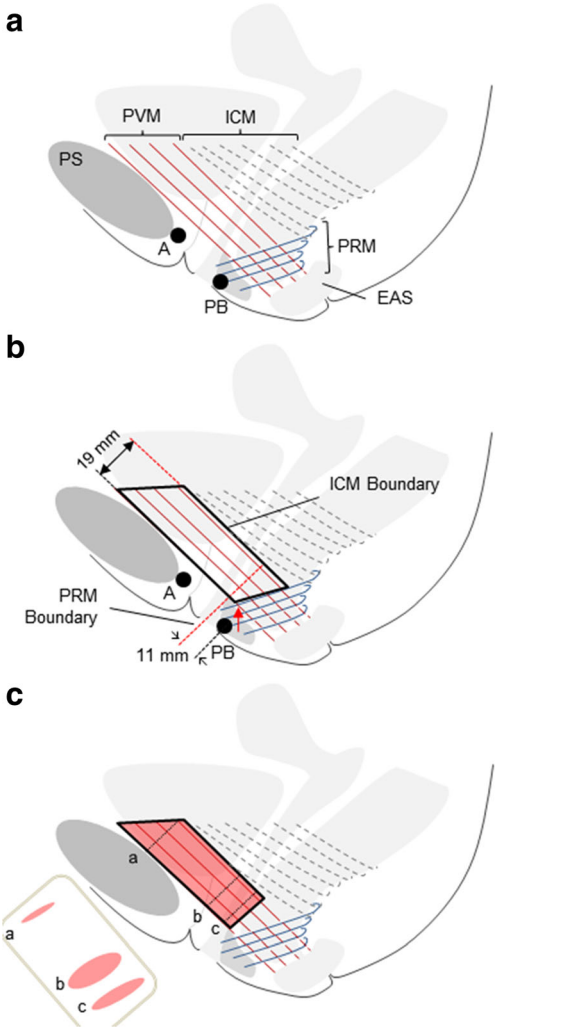

Fig. 1 **a** Lateral view of the female pelvis showing the pubic symphysis (PS), bladder, uterus, vagina, rectum, and anal sphincter. The pubovisceral (PVM), iliococcygeal (ICM), and puborectal (PRM) muscles are shown with their distinct line-of-action directions. *Point A* represents the arcuate pubic ligament and *point PB* the anterior wall of the perineal body. **b** The *black box* represents the extent of the natural muscle boundaries, including the ventral (19 mm) and dorsal (11 mm) boundaries of the PVM, avoiding overlap with the PVM and ICM. The red arrow points where the PRM overlaps the PVM, *dotted red lines* ICM and PRM boundaries. **c** PVM volume of interest is shaded in *red*, and *a*, *b*, and *c* represent selected transverse planes of this volume. *Cross-section b* is the maximum cross-sectional area

Materials and methods

This is a secondary analysis of a convenience sample of all women in our database with the unique characteristics of a unilateral PVM tear or having had a C-section. They represent women with unique and specific characteristics, so the sample size was determined by what was available. We were not comparing measurements, so a power calculation was not part of our study design. Eleven parous women with a complete unilateral levator ani tear were identified in whom the intact or slightly injured levator muscle present on one side could directly be compared with a damaged levator muscle on the other side (i.e., women with levator score 3-1 and 3-0 were included). Assuming that it is mostly the PVM rather than the PRM that is injured during birth [12], demarcation between these two overlapping muscles was evaluated by comparing the intact side with the contralateral side with the missing PVM. To do this, we compared the side that contained the intact PVM, PRM, and ICM with the side on which the PVM was missing. The portion of muscle seen on the intact side allowed us to define each boundary between this muscle and the two adjacent muscles—namely, the ICM and PRM. These scans were available from the Organ Prolapse and

Levator (OPAL II) case–control study of women with POP with protrusion below the hymen and no prior surgery for prolapse [13]. Women who served as controls were asymptomatic research volunteers with normal support (i.e., no prolapse to the level of the hymen) upon examination; they were recruited to be of similar age, parity, and hysterectomy status. Because, at least theoretically, intact muscle position might be altered by the injury on the contralateral side, we examined women who had not given birth vaginally. Scans were available from the Evaluating Maternal Recovery from Labor and Delivery (EMRLD) study [14] from 24 primiparous women 8 months postpartum who delivered by C-section. They had normal muscles unaltered by vaginal birth and had neither a PVM tear nor prolapse on the Pelvic Organ Prolapse Quantification (POP-Q) examination: seven women who had an elective C-section were used for method development, and all 24 women who had either an elective or with active second stage of labor C-section were used to calculate PVM CSA (Table 1). A secondary analysis of this convenience sample was performed instead of recruiting and scanning a new set of women due to the cost associated with the additional MRIs. Both studies were approved by the University of Michigan Institutional Review Board. These scans were used for the purposes of obtaining the CSA of normal muscles.

MRI images were obtained with a 3-T scanner (Achieva™, Philips Healthcare) with an eight-channel cardiac coil positioned over the pelvis. Images included coronal, axial, and sagittal proton-density–weighted (TR/TE 2100–2500/30 ms) sequences (field of view 20 cm; matrix 256 × 25; number of signal averages 2; slice thickness 4 mm; gap 1 mm). Additional 2-mm sections with 0.2-mm gaps in the axial and coronal planes were obtained with proton-density–weighted sequences (TR/TE 2100–2500/30 ms) [15]. The 2-mm scans were used primarily for cross-sectional measurements and the others for navigating general pelvic architecture. MRIs were imported into 3D Slicer (v. 4.5.0), so slices containing the volume of interest could be identified in a plane perpendicular to their muscle direction. The captured images were then exported into Image J (v.1.50i) for measurement, because measurements are not possible in 3D Slicer in reformatted planes.

Defining PVM boundaries

To identify a plane perpendicular to the PVM, its line of action was first established as a plane between origin and insertion—namely, the inner surface of the pubic bone and its insertion into the perineal structures. The boundary between the PVM and PRM (PRM boundary) and the PVM boundary with the ICM (ICM boundary) were then identified (Figs. 1 and 2i, ii). The following protocol was used to examine the PVM in women with a unilateral tear in which one side had an intact PVM and the other was missing (Fig. 2iii); note that both PRM and ICM can be seen (Fig. 2iv, v).

1. Identify PVM line of action in a parasagittal section using the following factors: (1) direction of visible striations within the muscle (Fig. 3), (2) knowledge that the muscle passes from the inner surface of the pubis to the vagina, perineal body, and anal sphincter complex, and (3) the lower boundary of the muscle lies against the perineal membrane.
2. Rotate the coronal plane to lie perpendicular to the PVM line of action.
3. Identify the PRM boundary by moving the plane back and forth and comparing the side with missing PVM to the side with intact muscle. The boundary was considered to occur where PRM mass is seen on the side where the PVM was absent (Fig. 2iv). The perineal body was selected as a reference structure for boundary location measurements, because it was consistently present and visible in all women whether or not a defect was present.
4. Identify the anterior aspect of the perineal body in a midsagittal plane. Then, find its location in the coronal plane and measure its distance from the identified PRM boundary.
5. Using the same rationale, identify the ICM boundary by moving the plane back and forth comparing the side with missing muscle with the side with intact muscle (Fig. 2v). The arcuate pubic ligament was chosen as the reference structure from which measurements of boundary location are made.

Table 1 Overview of participation by protocol phase, method development: boundary identification, measurements, and inter- and intrarater reliability

Group	No.	Method development: boundary identification	PVM CSA measured	Measurements and inter- and intrarater reliability	
				1st measurement	2nd measurement
Unilateral tear	11	Yes	No	No	No
C-section					
Elective C-section	7	Yes	Yes	Yes	Yes
C-section with 2nd stage	17		Yes	Yes	Yes

Each rater performed both the 1st and 2nd measurement. Only data from the first measurement is reported

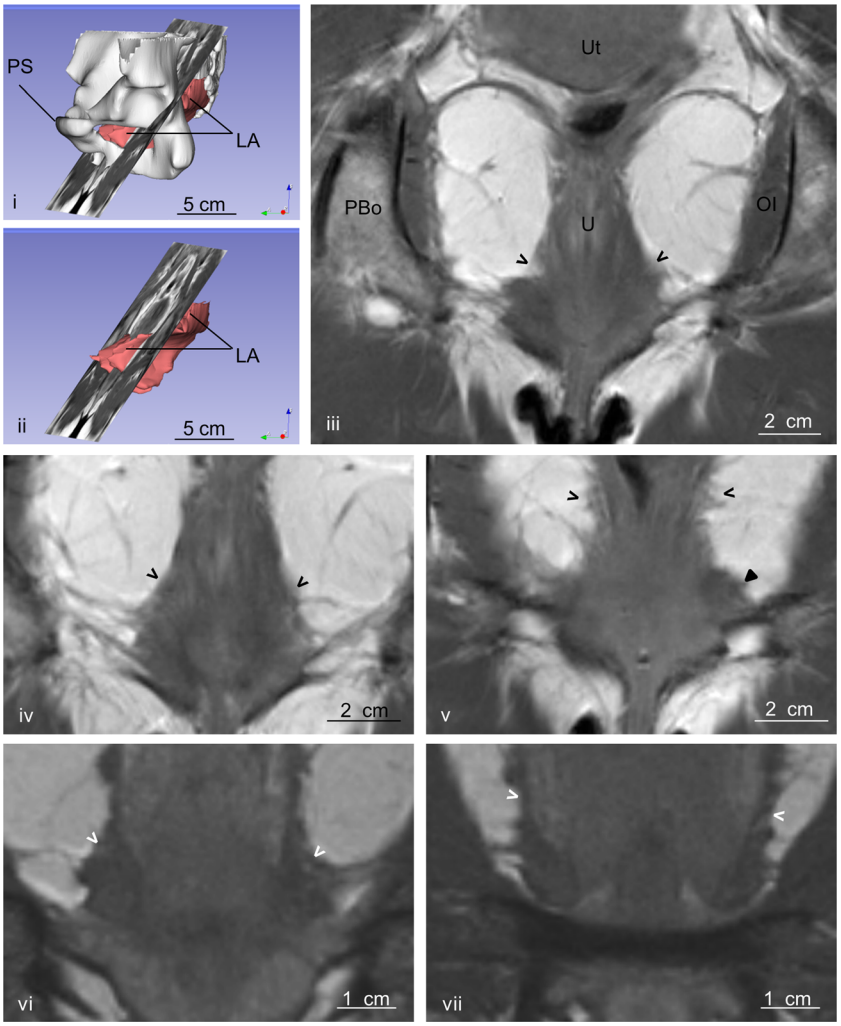

Fig. 2 Magnetic resonance image (MRI) of a healthy woman (i, ii, vi, vii) and of a woman with unilateral tear (panel iii–v). *Panels iii–vii* are in the coronal tipped plane. *i* is a 3D representation of the coronal plane rotated to the angle normal to the fiber direction (tipped plane), where pubic symphysis (PS) and levator ani (LA) are shown. *ii* is a 3D representation of LA and coronal tipped plane. *iii* Healthy pubovisceral muscle (PVM) on the *right side*, with absence of muscle on the *left side* of the image (both features indicated by *arrowheads*), where *PBo* denotes pubic bones, *Ut* uterus, *U* urethra, *OI* obturator internus. *iv* When moving back and forth on the coronal-tipped plane, there is a point where the puborectal muscle (PRM) is visible and intact on both sides. This point is located 11 mm ventral to the anterior aspect of the perineal body. *v* The PVM is absent on the left side but visible on the right side (*filled arrowhead*), the iliococcygeal muscle (ICM) is visible on both sides (*arrowheads*). The ventral boundary of the PVM is located 19 mm ventral to the arcuate pubic ligament. *vi* PRM in a healthy individual (*arrowheads*), but muscle morphology is different than that seen in *vii*. This subtle difference allows separation between both portions of the levator ani in healthy individuals. *vii* PVM transition to ICM in healthy individual (*white arrowheads*), seen as a small indentation cranial to the PVM belly

6. Using the first scan where the arcuate pubic ligament is seen when moving posterior–anterior, place a ruler perpendicularly from the arcuate pubic ligament to the identified boundary and measure the distance.

Because the absence of muscle unilaterally might lead to a distorted anatomy, we then applied this technique to women who had undergone elective C-section and whose muscles were normal on MRI. Using the insights gained from the unilateral set, it was possible to identify anatomical features of boundaries in intact muscles based on visible features: (1) for the PRM boundary, there was a different fiber organization in the muscle belly (Fig. 2vi); (2) for the ICM boundary, a small indentation was seen in the muscle belly "separating" the ICM from the PVM (Fig. 2vii). Next, we developed a measurement system that would first identify the PVM injury zone that precluded inadvertent overlap from the ICM and PRM. Distances of both PRM and ICM boundaries to the anatomical reference points were measured for all women in the method development phase (Table 1). The mean distance for the PRM boundary was 11 mm ventral to the anterior aspect of the perineal body and 19 mm cranial to the arcuate pubic ligament for the ICM boundary.

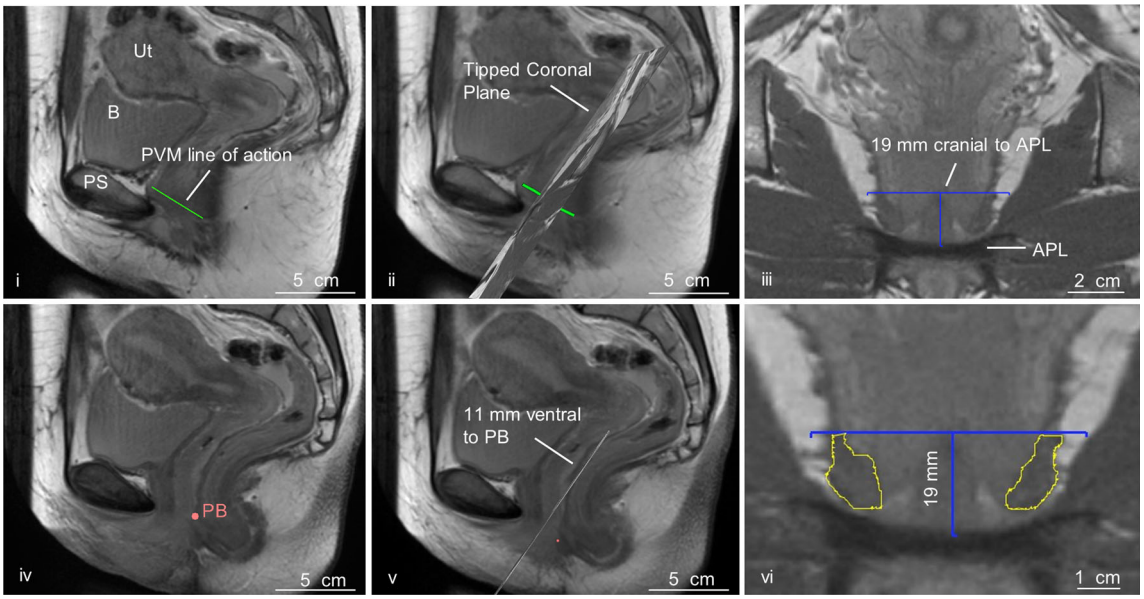

Fig. 3 Magnetic resonance images (MRI) of a healthy woman showing the different steps used to calculate the pubovisceral muscle (PVM) cross-sectional area (CSA). *i* Parasagittal plane showing PVM direction (*green line*), where *PS* pubic symphysis, *B* bladder, *Ut* uterus. *ii* 3D view of the sagittal plane and the tipped coronal plane, rotated to an angle normal to the PVM direction. *iii* Coronal plane, with tracing of ventral limit of the PVM, located 19 mm ventral to the arcuate pubic ligament (APL). *iv* Midsagittal plane showing location of anterior aspect of the perineal body (PB). *v* Tipped coronal plane moved to be 11 mm ventral to PB. *vi* PVM CSA tracing

Measurement of maximum PVM cross-sectional area in the injury zone

The protocol to measure the maximum PVM cross-section in the injury zone using 3D Slicer (steps 1–7) and Image J (steps 8 and 9) was as follows:

1. Import and align the three standard orthogonal imaging planes (i.e., axial, sagittal, coronal).
2. Identify the PVM line of action (Fig. 3i) in a parasagittal plane.
3. Rotate the coronal plane perpendicular to PVM line of action (Fig. 3ii).
4. Identify the arcuate pubic ligament; move the coronal plane (as in step 2) posterior–anterior to find the first plane in which the ligament is seen (Fig. 3iii).
5. Draw a line 19-mm long perpendicular to the arcuate pubic ligament (Fig. 3iii).
6. In a sagittal view, identify the anterior aspect of the perineal body (Fig. 3iv).
7. Place the coronal plane to show that same structure (anterior aspect of the perineal body) and move it 11 mm ventrally (Fig. 3v).
8. Outline the muscle bilaterally in every slice until the PVM arises from the pubic bone (include the slice defined in step 7) (Fig. 3 vi).
9. From the outlined PVM CSA, select the largest as the maximum PVM CSA.

For intrarater repeatability, measurements made by each examiner during two different sessions separated by ~2 weeks were used. For interrater repeatability, and for reporting measurements, the PVM CSA data from the first of these two sessions were used (Table 1).

Statistical analysis

To assess maximal PVM CSA, measurements of both left and right CSA where considered for each woman, and the largest of the pair was selected for statistical analysis.

To find inter- and intrarater reliability, paired *t* tests were used to assess differences between raters and left and right CSA. Intraclass correlation coefficients (ICC) (mode: two-way random; type: absolute agreement) [95% confidence interval (CI)] [16] were used to assess measurement agreement between raters and within a rater over time. All statistical analyses were conducted using SPSS (version 23, IBM, Chicago, IL, USA); $p < 0.05$ indicated statistical significance. All data are reported as mean and standard deviation (± SD), and percentiles were calculated for area measurements.

Results

Based on the analysis of women with unilateral tears and women who had an elective C-section used for method development (Table 2), the PRM boundary was a mean of 10.7 (±

Table 2 Participant demographics by group: unilateral tear and C-section (elective C-section and C-section with second stage of labor)

Group	No.	Age (years)	BMI (kg/m^2)	Vaginal deliveries	Duration 2nd stage of labor (min)	Time from birth to scanning (months)
Unilateral tear	11	57.0 (± 7.9)	25.1 (± 4.1)	2 (1, 2)	NA	> 60
C-section	24	28.9 (± 6.4)	27.0 (± 6.9)	0	228 (± 176)	8.1 (± 2.2)
Elective C-section	7	29.4 (± 5.1)	25.2 (± 5.0)	0	0	8.2 (± 1.9)
C-section with 2nd stage	17	28.6 (± 6.9)	27.8 (± 7.4)	0	322 (± 116)	8.1 (± 2.3)

No data were available (NA) for the duration of the second stage of labor for women with a unilateral tear. Data are presented as mean (± standard deviation), except for parity, which is presented as median (interquartile range)

5.1) mm ventral to the anterior aspect of the perineal body (median = 11 mm). The mean distance to the ICM boundary was 18.9 (± 3.5) mm cranial from the dorsal limit of the arcuate pubic ligament (median = 19 mm).

The average PVM line of action inclination angle to the horizontal reference plane corrected for variations in pelvic tilt [17] was 33° (± 5, range 21–43) in the 24 women who had undergone C-section (Table 2). Mean maximum PVM CSA in the injury zone for the 24 participants, all with intact PVM, was 1.25 cm^2 (± 0.29, range 0.75–1.86, CV 0.23). The 5th, 50th, and 95th percentiles were calculated as 0.77, 1.23, and 1.80 cm^2, respectively. No significant difference in maximum PVM CSA was found between left and right muscles (1.18 ± 0.28 cm^2 vs 1.15 ± 0.32 cm^2, $p = 0.46$). The PVM belly, as assessed by maximum unilateral PVM CSA, was located a mean 7.3 mm (± 8.0, range 0.0–30.0) and 6.5 mm (± 6.8, range 0.0–28.7) from the PRM boundary on the right and left sides, respectively.

In assessing interrater reliability, direct measurements of maximum PVM cross-section for each side were possible in all scans for both raters. Measurements between raters had an ICC of 0.95 (95% CI 0.90–0.98, $p = 0.29$) at the first time point and ICC of 0.89 (95% CI 0.80–0.95, $p = 0.15$) at the second time point. The intrarater assessment for each rater was also similar when comparing the two measured time points (ICC 0.89, 95% CI 0.75–0.95, $p = 0.09$) and (ICC 0.90, 95% CI 0.79–0.95, $p = 0.24$). The difference between the PVM CSA measurements for each of the two raters was 6 ± 4%.

Discussion

This paper describes a new method for directly measuring maximum anatomic PVM CSA on MRI. It provides a way to quantify muscle bulk in the physiologically appropriate manner: directly from the MRI using a plane that is normal to the recently described PVM line of action and muscle fiber direction [18] in the physiologically important thickest part of the muscle and avoids the artifacts introduced by the multistep process of model creation and measurement. The maximum PVM CSA measured in the injury zone represents the maximum isometric force that the PVM can generate based on its pubic bone insertion, whether the force transmission is normal or abnormal due to injury and compensated via lateral force transmission of adjacent structures.

Two difficulties arise in attempting to measure the CSA of the PVM. First, the PVM blends anatomically with the neighboring ICM without a well-defined separating fascia to signal the transition from one to the other. Second, the PVM lies immediately adjacent to and overlaps the PRM in its dorsal portion. Therefore, it was necessary to develop a method that allows a standard volume of PVM to be identified in which to seek its maximum CSA: that was the goal of our study. Lack of such a method has led to the wide variations reported in PVM area [11, 19, 20] and thickness [8, 21, 22] measurements. In addition, specific anatomical landmarks that remain visible even in the absence of the PVM were used to identify the location where it does not overlap with the ICM or PRM. This is the first time this separation has been made. Prior studies used planes of separation that were defined based on static anatomical landmarks but not derived from actual measurements made. By using measured distances to define PVM anatomical boundaries, it is possible to identify its expected location even when it is missing. The acceptable intra- and interrater reliability for this analysis indicates that it is possible to achieve consistent results in measuring maximum PVM CSA.

Maximum unilateral PVM CSA values presented here are substantially smaller than published values based on lofted model measurement techniques (e.g., present value of 1.25 (± 0.29) cm^2 vs 2.44 cm^2 [11] and 4.06 cm^2 [19]). We believe these differences result from different measurement techniques and protocols. Specifically, because area measurements in our study were made orthogonal to the PVM line of action using a protocol that separates the PVM from the adjacent PRM and ICM, we believe measurement artifacts to be smaller and that inclusion of PRM mass within the measured area was avoided: the location of maximum CSA, whether on the left or right side, was at least 6 mm ventral to the PRM boundary. We found the CV in PVM CSA to be similar to that found in other small striated muscles with parallel fibers, such as the lumbar multifidus [23].

The recent description of MRI measurement techniques to determine the true PVM line of action [18] was fundamental to the accuracy of the orthogonal measurements obtained in this study. In addition, this study has allowed us to recognize that the PVM CSA varies along its length, much as the biceps muscle does, with the CSA being much smaller near its pubic origin, presumably due to higher type 1 collagen content at the pubic aponeurosis [24]. The method described here allows maximal PVM CSA to be identified as one moves distally in the muscle, and some images distinctly show that the muscle has a belly.

The definition of PVM boundaries was based on three different concepts: the first is the angle of its fiber orientation and hence its line of action, and the other two are the definition of its boundaries with the ICM and PRM. The measured PVM angle of fiber direction was smaller than that reported by Betschart et al. (33 ± 5° vs 41 ± 8°) [18]. Our study identified the direction of striations within the muscle, while Betschart selected scans in which muscle fibers were visible—a feature not consistent in all women. A simple trigonometric calculation shows a difference of 8° would result in 1% change in maximum measured unilateral PVM CSA, so this difference is likely not important.

Boundaries of the injury zone were calculated as being 19 mm cranial from the dorsal limit of the arcuate pubic ligament for the ICM boundary and 11 mm ventral to the anterior aspect of the perineal body for the PRM boundary, with maximum anatomic PVM CSA being measured within these limits. However, in women smaller than those measured in our study, there is a risk this might lead to inclusion of the small portions of the ICM and/or PRM. Conversely, in a very large woman, one might underestimate the PVM anatomic CSA. The magnitude of this potential effect can be addressed in the future when larger sample sizes make this type of analysis possible. Clearly, with a larger sample size, the values we report for the 5th and 95th percentile CSA might be expected to be conservative, but the mean value should not change greatly.

The ability to make measurements directly from MRI rather than outlining the muscle and creating a 3D model of the PVM is a strength of the measurement protocol reported here. A limitation of this technique-development study is the small sample size, the fact that it is not population based, that measurement of CSA does not inform about function and quality of outlined tissue (i.e., extent of fatty infiltration within the muscle), and how these characteristics change with age and PVM tear. However, neither the CSA [19] nor the maximum vaginal closure force [25] appear to be affected by age in nullipara, suggesting that intact muscle quality does not significantly change with age. In addition, the reliability studies were performed on images from the same individuals as those used for protocol development; however, these were the only individuals available with these unusual characteristics in our MRI database. We are not able to validate these measurements against a gold standard, because measuring the PVM CSA in cadaver specimens would not provide meaningful information for the living: the pelvic floor is too grossly distorted by loss of muscle tone after death [26]. Now that a technique for measuring muscle CSA is feasible and shows acceptable reproducibility, PVM CSA can be used to understand its interaction with the mechanisms of prolapse.

Acknowledgments We thank Bing Xie, MD, for her support in the data analysis portion of this paper. We also thank Janis M. Miller, PhD, the principal investigator for the EMRLD project, for generously allowing us to use those MRI scans. Finally, we thank the women who were willing to be tested for these studies.

Funding We are grateful for the Public Health Service and the Office for Research on Women and Gender Grants #P50 HD044406-07 and HD R01 38665 (JAAM & JOLD). MM was supported by the Fulbright Program for her masters dissertation research in Ann Arbor while a graduate student at the University of Porto, Portugal.

Compliance with ethical standards

Conflict of interest None.

References

1. DeLancey JOL. What s new in the functional anatomy of pelvic organ prolapse? Curr Opin Obstet Gynecol. 2016;28(5):420–9.
2. Kearney R, Sawhney R, DeLancey JOL. Levator Ani muscle anatomy evaluated by origin-insertion pairs. Obstet Gynecol. 2004;104(1):168–73.
3. Shafik A, Doss S, Asaad S. Etiology of the resting myoelectric activity of the levator ani muscle: Physioanatomic study with a new theory. World J Surg. 2003;27(3):309–14.
4. DeLancey JO, Morgan DM, Fenner DE, Kearney R, Guire K, Miller JM, et al. Comparison of levator ani muscle defects and function in women with and without pelvic organ prolapse. Obstet Gynecol. 2007;109:295–302.
5. Dietz HP, Simpson JM. Levator trauma is associated with pelvic organ prolapse. BJOG An Int J Obstet Gynaecol. 2008;115(8):979–84.
6. Chen L, Ashton-Miller JA, DeLancey JOL. A 3D finite element model of anterior vaginal wall support to evaluate mechanisms underlying cystocele formation. J Biomech. 2009;42(10):1371–7.
7. Kim J, Betschart C, Ramanah R, Ashton-Miller JA, DeLancey JOL. Anatomy of the pubovisceral muscle origin: macroscopic and microscopic findings within the injury zone. Neurourol Urodyn. 2014;1–7.
8. Alt C, Hampel F, Hallsheidt P, Shon C, Schele B, Brocker K. 3T MRI-based measurements for the integrity of the female pelvic floor in 25 healthy nulliparous women. Neurourol Urodyn. 2016;35:218–23.
9. Albrich SB, Laterza RM, Skala C, Salvatore S, Koelbl H, Naumann G. Impact of mode of delivery on levator morphology: a prospective observational study with three-dimensional ultrasound early in the postpartum period. 2011;51–61.
10. Enoka RM. Muscle strength and its development. New perspectives. Sports Med. 1988;6(3):146–68.
11. Chen L, Hsu Y, Ashton-Miller JA, DeLancey JOL. Measurement of the pubic portion of the levator ani muscle in women with unilateral defects in 3-D models from MR images. Int J Gynecol Obstet. 2006;92(3):234–41.
12. DeLancey JOL, Sørensen HC, Lewicky-Gaupp C, Smith TM. Comparison of the puborectal muscle on MRI in women with

POP and levator ani defects with those with normal support and no defect. Int Urogynecol J. 2012;23(1):73–7.
13. DeLancey JOL, Morgan DM, Fenner DE, Kearney R, Guire K, Miller JM, et al. Comparison of levator ani muscle defects and function in women with and without pelvic organ prolapse. Obstet Gynecol. 2007;109(2 Part 1):295–302.
14. Lisa Kane Low, Ruth Zielinski, Yebin Tao, Andrzej Galecki, Catherine J. Brandon, Janis M. Miller. Predicting Birth-Related Levator Ani Tear Severity in Primiparous Women: Evaluating Maternal Recovery from Labor and Delivery (EMRLD Study). Open Am J Obstet Gynecol. 2014;04(06):266–278.
15. Miller JM, Brandon C, Jacobson JA, Low LK, Zielinski R, Ashton-Miller J, et al. MRI findings in patients considered high risk for pelvic floor injury studied serially after vaginal childbirth. Am J Roentgenol. 2010;195(3):786–91.
16. Rankin G, Stokes M. Reliability of assessment tools in rehabilitation: an illustration of appropriate statistical analyses. Clin Rehabil. 1998;12(3):187–99.
17. Betschart C, Chen L, Ashton-Miller JA, DeLancey JOL. On pelvic reference lines and the MR evaluation of genital prolapse: a proposal for standardization using the pelvic inclination correction system. Int Urogynecol J. 2013;18(9):1199–216.
18. Betschart C, Kim J, Miller JM, Ashton-Miller JA, DeLancey JOL. Comparison of muscle fiber directions between different levator ani muscle subdivisions: in vivo MRI measurements in women. Int Urogynecol J Pelvic Floor Dysfunct. 2014;25(9):1263–8.
19. Morris VC, Murray MP, DeLancey JOL. Ashton-miller JA. A comparison of the effect of age and levator ani and obturador internus muscle cross-sectional areas and volumes in nulliparous women. Neurourol Urodyn. 2012;31:481–6.
20. Ackerman AL, Lee UJ, Jellison FC, Tan N, Patel M, Raman SS, et al. MRI suggests increased tonicity of the levator ani in women with interstitial cystitis/bladder pain syndrome. Int Urogynecol J Pelvic Floor Dysfunct. 2016;27(1):77–83.
21. Hoyte L, Jakab M, Warfield SK, Shott S, Flesh G, Fielding JR. Levator ani thickness variations in symptomatic and asymptomatic women using magnetic resonance-based 3-dimensional color mapping. Am J Obstet Gynecol. 2004;191(3):856–61.
22. Fielding JR, Dumanli H, Schreyer AG, Okuda S, Gering DT, Zou KH, et al. MR-based three-dimensional modeling of the normal pelvic floor in women: quantification of muscle mass. Am J Roentgenol. 2000;174(3):657–60.
23. Sasaki T, Yoshimura N, Hashizume H, Yamada H, Oka H, Matsudaira K, et al. MRI-defined paraspinal muscle morphology in Japanese population: the Wakayama spine study. PLoS One. 2017;12(11):1–15.
24. Kim T, Sridharan I, Ma Y, Zhu B, Chi N, Kobak W, et al. Identifying distinct nanoscopic features of native collagen fibrils towards early diagnosis of pelvic organ prolapse. Nanomedicine. 2015;12(3):667–75.
25. Trowbridge ER, Wei JT, Fenner DE, Ashton-Miller JA, DeLancey JOL. Effects of aging on lower urinary tract and pelvic floor function in nulliparous women. Obstet Gynecol. 2007;109(3):715–20.
26. Lebendige RK. Anatomie der Vagina. Geburtshilfe Frauenheilkd. 1966;26:1213–23.